Antiferromagnetic ordering and estimation of the exchange interaction in the π-d system λ-(BEDSe-TTF)$_2$FeCl$_4$ studied using ^{13}C NMR

Rikumaru Saito,[1] Takuya Kobayashi,[2] Hiromi Taniguchi,[2] Shuhei Fukuoka,[1] and Atsushi Kawamoto[1,*]
[1]*Department of Condensed Matter Physics, Graduate School of Science, Hokkaido University, Sapporo 060-0810, Japan*
[2]*Graduate School of Science and Engineering, Saitama University, Saitama 338-8570, Japan*

(Received 21 July 2023; accepted 30 August 2023; published 9 October 2023)

We performed ^{13}C NMR measurements on λ-(BEDSe-TTF)$_2$FeCl$_4$[BEDSe-TTF = bis(ethylenediseleno) tetrathiafulvalene] to investigate the antiferromagnetic transition in this material and evaluate the exchange interaction $J_{\pi d}$ between the donor molecules and $FeCl_4^-$ anions. Based on the NMR spectrum and the nuclear spin-lattice relaxation rate, we determined that the antiferromagnetic transition in the donor layers occurs at 25 K. The structure of the NMR spectra in the antiferromagnetic phase resembles that of λ-(BEDSe-TTF)$_2$GaCl$_4$. We used the angle dependence of the NMR shift in the paramagnetic phase and the experimentally determined demagnetization factor to estimate $J_{\pi d}$ of λ-(BEDSe-TTF)$_2$FeCl$_4$ as 3.4(7) T/μ_B . This result shows that the π-d interaction of λ-(BEDSe-TTF)$_2$FeCl$_4$ is weaker than that of λ-(BETS)$_2$FeCl$_4$. The different signs of $J_{\pi d}$ between λ-(BEDSe-TTF)$_2$FeCl$_4$ and λ-(BETS)$_2$FeCl$_4$ could be attributed to the different paths for the π-d interaction in the two systems.

DOI: 10.1103/PhysRevB.108.155112

I. INTRODUCTION

Quasi-two-dimensional organic conductors have attracted considerable attention because of their rich phase diagrams, which exhibit superconducting, magnetic-ordered, and charge-ordered states, among others [1]. The crystal structure of these conductors consists of alternating conducting layers formed by donor molecules, as shown in Fig. 1(a), and insulating layers formed by anions. Introducing magnetic ions, such as $FeCl_4^-$ with $S = 5/2$, into the anion layers causes π-d interactions between the conduction electrons with $S = 1/2$ and the localized 3d spins, resulting in the emergence of fascinating physical properties. Among several π-d systems, λ-type salts have attracted interest because of their diverse physical properties. As shown in Fig. 1(b), the dimerization of two donor molecules in λ-type salts creates in an effective half-filled system.

The well-known π-d system λ-(BETS)$_2$FeCl$_4$[BETS = bis(ethylenedithio)tetraselenafulvalene] exhibits superconductivity (SC) under a magnetic field. This compound exhibits an antiferromagnetic (AF) transition accompanied by a metal-insulator (MI) transition in the absence of a magnetic field [2–4]. In the early studies, the AF transition was thought to occur for localized 3d spins and the π-electron systems responsible for electrical conduction caused the material to become an insulator. However, specific heat measurements revealed a Shottky-type anomaly because of the existence of 3d spin degrees of freedom below the transition temperature [5,6]. This result indicates that the AF ordering is not caused by 3d spins but π spins. Hereafter, this picture is called the π ordering model. Within this model, magnetic ordering occurs in the π-electron systems and a similar magnetic transition should be observed in the isostructural nonmagnetic λ-(BETS)$_2$GaCl$_4$. However, λ-(BETS)$_2$GaCl$_4$ undergoes a superconducting transition and cannot serve as a reference system for λ-(BETS)$_2$FeCl$_4$ [2,7,8]. The MI transition in λ-(BETS)$_2$FeCl$_4$ complicates the AF transition mechanism. To study the mechanism of the AF transition, including the role of the π-d interaction in this transition, it is useful to compare the behavior of Fe and Ga salts is based on λ-type salts with the same ground state.

λ-(STF)$_2$FeCl$_4$ and λ-(STF)$_2$GaCl$_4$[BEDT-STF (STF) = bis(ethylenedithio)diselenadithiafulvalene] are insulators over the entire considered temperature range because of the negative pressure effect of donor substitution on the MI transition [9–11]. The π-electron systems of λ-(STF)$_2$FeCl$_4$ were investigated by ^{13}C NMR (nuclear magnetic resonance). The AF transition in the donor layers was found to occur at 16 K [12]. The 3d spin systems were investigated by ^{57}Fe Mössbauer spectroscopy, and multistep development of the hyperfine fields was observed below 16 K [13]. Heat capacity measurements revealed a Schottky-type anomaly similar to that observed in λ-(BETS)$_2$FeCl$_4$, indicating that the 3d spins in λ-(STF)$_2$FeCl$_4$ also behave as paramagnetic spins [14]. Unfortunately, λ-(STF)$_2$GaCl$_4$ did not undergo the AF transition down to 0.3 K [15–17]. In λ-(ET)$_2$GaCl$_4$[ET = bis(ethylenedithio)tetrathiafulvalene] located on the side of the phase diagram with a more negative pressure, the AF transition has been observed at 13 K by ^{13}C NMR [18]; however, λ-(ET)$_2$FeCl$_4$ was not been available for use in the present study.

These differences between the ground states of Fe and Ga salts have made it difficult to understand the π-d interaction. Thus, we investigated BEDSe-TTF salts [BEDSe-TTF = bis(ethylenediseleno)tetrathiafulvalene]. ^{13}C NMR

*atkawa@sci.phys.hokudai.ac.jp

measurements on λ-(BEDSe-TTF)$_2$GaCl$_4$ showed that the AF transition occurred at 22 K [19]. We have reported ^{57}Fe Mössbauer measurements and magnetic susceptibility measurements on λ-(BEDSe-TTF)$_2$FeCl$_4$ [20]. Although the Mössbauer measurements indicated multistep development of the internal field exerted on Fe sites below 26 K, the magnetic susceptibility measurements did not indicate a magnetic anomaly at this temperature. As the field development was almost identical to that of λ-(STF)$_2$FeCl$_4$, except for the temperature at which the hyperfine fields started to develop, we concluded that the AF transition in donor layers occurred even in λ-(BEDSe-TTF)$_2$FeCl$_4$. Hence, ^{13}C NMR measurements need to be performed on λ-(BEDSe-TTF)$_2$FeCl$_4$ to investigate the magnetism of the π electrons because ^{57}Fe Mössbauer measurements probe the magnetism of 3d electrons and not π electrons.

It is important to evaluate the coupling parameter between the π and 3d spins, $J_{\pi d}$, to understand the π-d interaction. In a previous study, we compared the strengths of the π-d interaction between λ-(BEDSe-TTF)$_2$FeCl$_4$ and λ-(BETS)$_2$FeCl$_4$ [20]. We observed weak anisotropy of the magnetic susceptibility in λ-(BEDSe-TTF)$_2$FeCl$_4$ [20]. By contrast, clear anisotropy was reported for λ-(BETS)$_2$FeCl$_4$ and λ-(STF)$_2$FeCl$_4$ [3,11]. The weak anisotropy observed in λ-(BEDSe-TTF)$_2$FeCl$_4$ was similar to that in λ-(BETS)$_2$FeBr$_x$Cl$_{4-x}$ with $0.3 < x < 0.5$, and the Weiss temperature of λ-(BEDSe-TTF)$_2$FeCl$_4$ of 7.4 K was also smaller than that of 15 K for λ-(BETS)$_2$FeCl$_4$ [21]. These results suggested that the π-d interaction in λ-(BEDSe-TTF)$_2$FeCl$_4$ is weaker than that in λ-(BETS)$_2$FeCl$_4$. However, there has been no quantitative evaluation of $J_{\pi d}$ in λ-(BEDSe-TTF)$_2$FeCl$_4$.

For λ-(BETS)$_2$FeCl$_4$, $J_{\pi d}$ could be estimated from the field-induced superconductivity (FISC), which can be explained by the Jaccarino-Peter compensation mechanism [22]. Whereas λ-(BETS)$_2$FeCl$_4$ exhibits an MI transition at zero or small fields, the salt exhibits metallic behavior with increasing magnetic field strength and superconductivity above 18 T [23,24]. When a large external field is applied parallel to the conducting layers, paramagnetic 3d spins align in the direction of the external field and exert an exchange field on the π electrons. The magnetic field exerted on the π electrons is canceled out, resulting in the emergence of superconductivity. The maximum transition temperature is 4.2 K at 33 T corresponding to complete cancellation of the magnetic field exerted on the π electrons [24].

NMR is a microscopic magnetic probe that is suitable for evaluating $J_{\pi d}$. In addition, $J_{\pi d}$ of λ-(BETS)$_2$FeCl$_4$ can be estimated from ^{77}Se NMR measurements [25]. This estimate corresponds to $|H_{\rm exch}| = 32 \pm 2$ T. Hence, $J_{\pi d}$ of λ-(BETS)$_2$FeCl$_4$ is estimated as -6.6 T/μ_B . Within this approach, the estimation of $J_{\pi d}$ strongly depends on the demagnetization factor corrected for the crystal shape. In the studies on λ-(BETS)$_2$FeCl$_4$ and λ-(STF)$_2$FeCl$_4$, the demagnetization factor was calculated using the ellipsoid approximation for a thin rectangular crystal with fixed dimensions [25,26]. The demagnetization factor was not taken into account in a study on κ-(BETS)$_2$FeBr$_4$ [27]. The mosaic structure of an object crystal could also contribute to the demagnetization factor. The difficulty of estimating the demagnetization factor introduces ambiguity into the evaluation of $J_{\pi d}$. Hence, to the quantitative evaluate $J_{\pi d}$, the demagnetization factor should be determined experimentally.

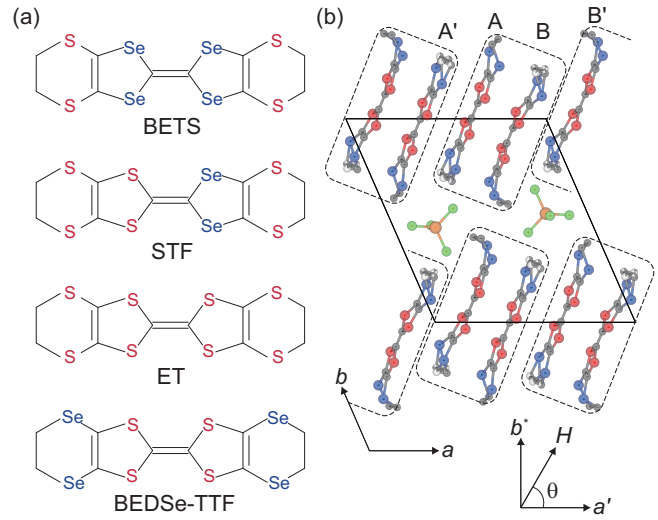

FIG. 1. (a) Structures of donor molecules of BETS, STF, ET, and BEDSe-TTF. (b) Crystal structure of λ-(BEDSe-TTF)$_2$FeCl$_4$. The dimer is surrounded by a dashed curve. The A and B molecules are crystallographically independent, and the A′ and B′ molecules are equivalent to the A and B molecules, respectively, and connected by inversion symmetry.

In this study, we performed ^{13}C NMR measurements on λ-(BEDSe-TTF)$_2$FeCl$_4$. ^{13}C NMR measurements can selectively probe π-electron systems. We measured the temperature dependence of the NMR spectra and nuclear spin-lattice relaxation rate ($1/T_1$) to investigate the magnetic properties of the π-electron systems. To verify the weak π-d interaction, we evaluated $J_{\pi d}$ from the angle dependence of the ^{13}C NMR measurements using the experimentally determined demagnetization factor.

II. EXPERIMENTS

Single crystals of λ-(BEDSe-TTF)$_2$FeCl$_4$ were prepared by electrochemical oxidation in a solution of the tetrabutylammonium salt, [n − Bu$_4$N]FeCl$_4$ in chlorobenzene with ^{13}C-enriched BEDSe-TTF, as shown in Fig. 2(a). To prevent spectrum splitting by nuclear spin-spin coupling, that is, the Pake doublet, one of the carbons in the central C-C bond in the BEDSe-TTF molecules was enriched with a ^{13}C isotope [19]. The samples were thin black rectangular crystals, where the ac plane had a well-developed surface with dimensions of $2 \times 0.2 \times \sim 0.06$ mm^3, as shown in Fig. 2(b). Next, ^{13}C

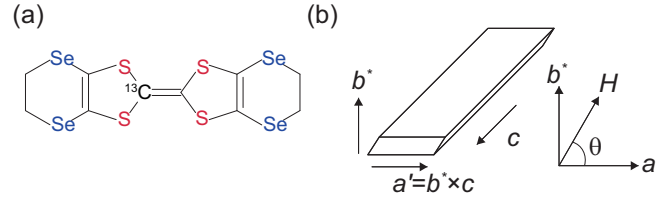

FIG. 2. (a) ^{13}C-enriched BEDSe-TTF molecule. (b) Crystal shape of λ-(BEDSe-TTF)$_2$FeCl$_4$.

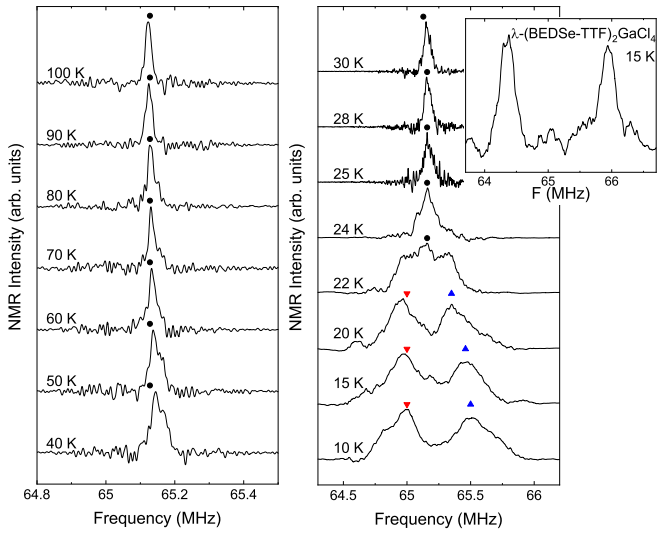

FIG. 3. Temperature dependence of the NMR spectra of λ-(BEDSe-TTF)$_2$FeCl$_4$ under a field with $H \parallel b^*$. The inset shows the NMR spectrum of λ-(BEDSe-TTF)$_2$GaCl$_4$ at 15 K under a field with $H \parallel b^*$.

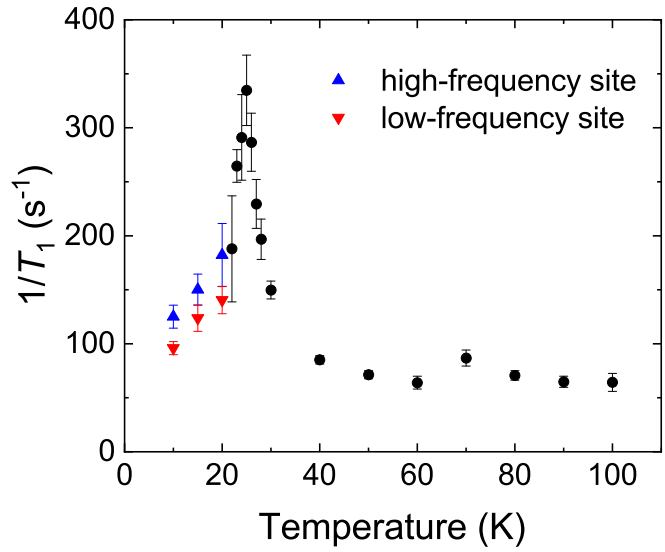

FIG. 4. Temperature dependence of $1/T_1$ of λ-(BEDSe-TTF)$_2$FeCl$_4$. The circle and triangle symbols correspond to the symbols shown in Fig. 3.

NMR measurements were conducted under a magnetic field of 6.1 T. NMR spectra were obtained using a fast Fourier transformation of the spin echo signal with a $\pi/2$-π pulse sequence. The typical width of a $\pi/2$ pulse is 1.5 μs. $1/T_1$ was estimated using the conventional saturation recovery method. The relaxation curves $M(t)$ could be fitted with a stretched exponential function described as $M(t) = M_0[1 - \exp(-t/T_1)^{\beta}]$ [19], where $M(t)$ is the nuclear magnetization, and M_0 is the equilibrium nuclear spin magnetization. We set the parameter β to 0.9 as in nonmagnetic Ga salt [19]. The temperature dependence of the spectra and $1/T_1$ were measured in the direction of $H \parallel b^*$. Spectra below 22 K were obtained by combining several spectra. For comparison, the spectrum of the AF phase of λ-(BEDSe-TTF)$_2$GaCl$_4$ was measured in the same configuration at 15 K. The angle dependence of the NMR shift of λ-(BEDSe-TTF)$_2$FeCl$_4$ and λ-(BEDSe-TTF)$_2$GaCl$_4$ was measured at 100 K, where the shifts were determined by fitting the spectra with a Lorentzian function. Figure 2(b) shows the definition of the angle and the rotation direction used in this study.

III. RESULTS AND DISCUSSION

A. AF transition at 25 K

Figure 3 shows the temperature dependence of the NMR spectra from 100 to 10 K obtained under a magnetic field parallel to the b^* axis. In λ-type salts, there are two crystallographically independent A and B molecules, as shown in Fig. 1(b). A′(B′) are equivalent to A (B) molecules connected by inversion symmetry. Each molecule has two nonequivalent ^{13}C sites, resulting in four crystallographically nonequivalent ^{13}C sites.

Although the four peaks are expected from crystallographic considerations, a single peak with fine structures is observed in the high-temperature range. The four peaks are merged into one peak because the hyperfine coupling constants are almost the same as the A and B molecules are almost parallel to each other and the two nonequivalent ^{13}C sites in the molecule are chemically equivalent. With decreasing temperatures, the spectrum broadens and shifts to a higher frequency because of magnetization of the 3d spins. Below 22 K, the aforementioned single peak splits into two broad peaks. This result suggests that the π-electron systems are antiferromagnetically ordered, generating an internal field at the ^{13}C sites. The inset of Fig. 3 shows the spectrum of the AF phase of λ-(BEDSe-TTF)$_2$GaCl$_4$ for the same configuration, which exhibits similar spectral splitting below a T_N of 22 K. The spectrum consists of two peaks similar to those of λ-(BEDSe-TTF)$_2$FeCl$_4$. These results indicate that the AF transition occurs in the π-electron systems as in λ-(BEDSe-TTF)$_2$GaCl$_4$ and the AF phase in both salts has simple up-down spin magnetic structure.

Figure 4 shows the temperature dependence of $1/T_1$ below 100 K. The symbols in Fig. 4 correspond to those shown in Fig. 3. $1/T_1$ remains almost constant above 40 K and increases steeply below 30 K. The emergence of the internal field and the divergence of $1/T_1$ toward 25 K confirm that the π-electron systems undergo the AF transition at 25 K.

The peak splitting in the spectra of both the Ga and Fe salts suggests that the magnetic ground state of the π-electron systems is the same in λ-(BEDSe-TTF)$_2$FeCl$_4$ and λ-(BEDSe-TTF)$_2$GaCl$_4$. The transition temperature of λ-(BEDSe-TTF)$_2$FeCl$_4$ is 3 K higher than that of λ-(BEDSe-TTF)$_2$GaCl$_4$. This result might indicate that the π-d interaction stabilizes the AF ordering of the π-electron systems. The ^{13}C NMR on λ-(STF)$_2$Fe$_x$Ga$_{1-x}$Cl$_4$ also showed that the transition temperature of the π-electron systems increases with the Fe content [26].

Figure 5 shows the temperature dependence of the hyperfine fields obtained by ^{13}C NMR and ^{57}Fe Mössbauer measurements. The closed and open symbols correspond to λ-(BEDSe-TTF)$_2$FeCl$_4$ and λ-(STF)$_2$FeCl$_4$, respectively. In

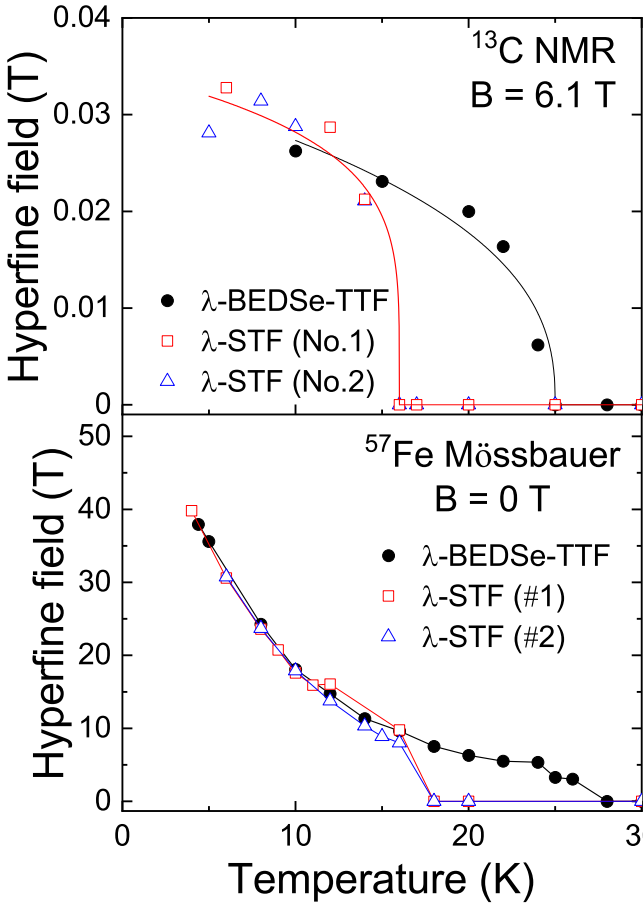

FIG. 5. Temperature dependence of the hyperfine fields of λ-(BEDSe-TTF)$_2$FeCl$_4$ and λ-(STF)$_2$FeCl$_4$ obtained by ^{13}C NMR and ^{57}Fe Mössbauer measurements [12,13,20]. λ-STF (#1) and λ-STF (#2) are different samples of the same compound.

the ^{13}C NMR measurements, the hyperfine fields are defined using the width of the split peaks in the spectrum. In the two measurements, the development of the hyperfine fields in λ-(BEDSe-TTF)$_2$FeCl$_4$ is similar to that in λ-(STF)$_2$FeCl$_4$, except for the temperature at which the hyperfine fields start to develop. Fitting the temperature dependence of the hyperfine field observed by ^{13}C NMRmeasurements with $B_{hf}(T) = A(1 - T/T_N)^{\beta}$ yielded $A = 0.033$ and $\beta = 0.4$ for λ-(BEDSe-TTF)$_2$FeCl$_4$ and $A = 0.034$ and $\beta = 0.2$ for λ-(STF)$_2$FeCl$_4$. The values of β for λ-(BEDSe-TTF)$_2$FeCl$_4$ and λ-(STF)$_2$FeCl$_4$ are very different. This is thought to be due to the fact that the AF phase of STF salts appears by introducing $3d$ spins. Although BEDSe-TTF salts undergo the AF transition, λ-(STF)$_2$GaCl$_4$ did not undergo the AF transition. The hyperfine fields increase suddenly at 25 K at the ^{13}C sites, but exhibits multistep behavior at the ^{57}Fe sites. These two different magnetization processes were also discussed in our previous study and are characteristic of insulating λ-FeCl$_4$ salts [12].

There are three types of magnetic interactions in λ-FeCl$_4$ salts,: $J_{\pi\pi}$, $J_{\pi d}$, and J_{dd}. $J_{\pi\pi}$ and J_{dd} are the coupling parameters between π spins and between $3d$ spins, respectively. The same order of magnitude is expected for $|J_{dd}/k_B|$ in λ-(BEDSe-TTF)$_2$FeCl$_4$ as for λ-(BETS)$_2$FeCl$_4$ because

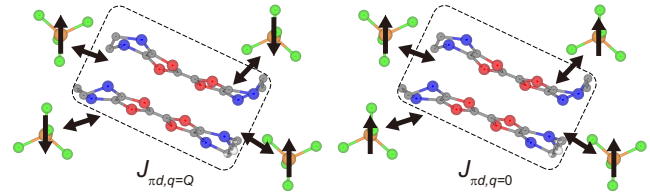

FIG. 6. Antiferromagnetic structure with $q = Q$ ($J_{\pi d,q=Q}$) and the ferromagnetic structure with $q = 0$ ($J_{\pi d,q=0}$). The two-headed arrows between a dimer and anions represent the π-d interaction.

the nearest Fe-Fe distance is almost the same. Assuming a $|J_{dd}/k_B|$ of 0.64 K, as suggested by the theoretical calculation on λ-(BETS)$_2$FeCl$_4$, yields an estimated transition temperature of 3.73 K based on mean-field theory [28]. This temperature is considerably lower than 25 K. Hence, the development of the hyperfine fields at the Fe sites at 26 K does not result from the spontaneous magnetization of the $3d$ spins, but from the passive polarization of the $3d$ spins through the π-d interaction of the antiferromagnetically ordered π-electron systems.

B. Estimation of $J_{\pi d}$ in λ-(BEDSe-TTF)$_2$FeCl$_4$

We measured the angle dependence of the NMR shift of BEDSe-TTF salts in the paramagnetic state to examine the weakened π-d interaction in λ-(BEDSe-TTF)$_2$FeCl$_4$, as suggested by the magnetic susceptibility under low magnetic fields. Figure 6 shows the two types of π-d interaction that are generally possible. The first type $J_{\pi d,q=Q}$ is defined as the AF structure with the wave vector $q = Q$, and the second type $J_{\pi d,q=0}$ is defined as the ferromagnetic structure with $q = 0$. $J_{\pi d,q=0}$ contributes to the FISC. In the paramagnetic state, the magnetic moments of Fe ions are parallel to the external field and the π-d interaction corresponds to $J_{\pi d,q=0}$.

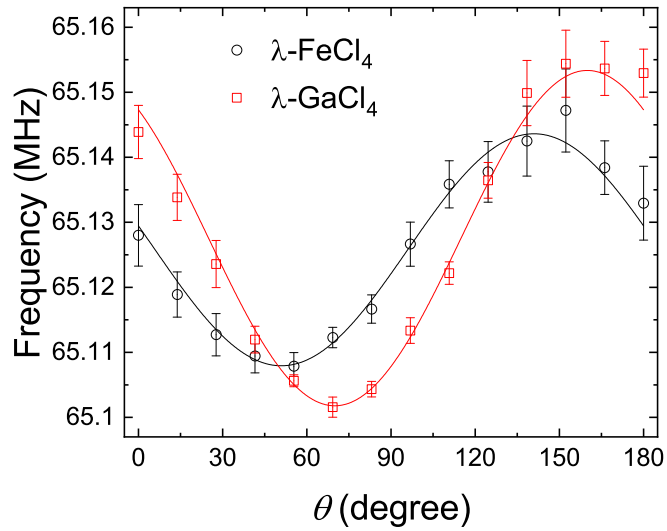

FIG. 7. Angle dependence of the NMR shift of λ-(BEDSe-TTF)$_2$GaCl$_4$ and λ-(BEDSe-TTF)$_2$FeCl$_4$ at 100 K. The solid lines are fits to the experimental data.

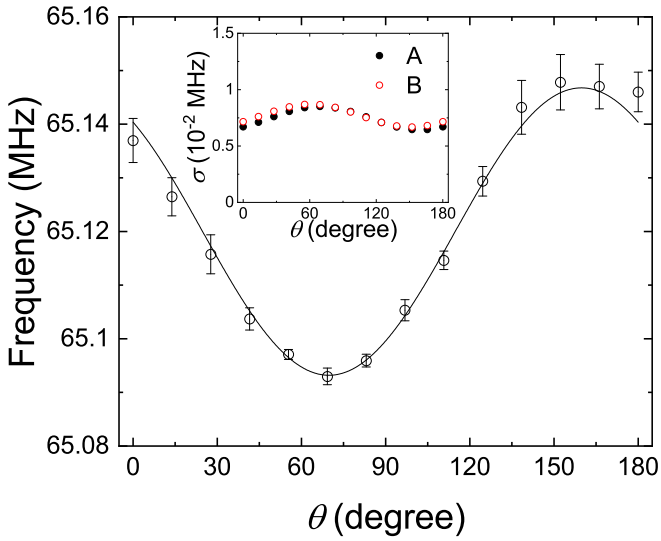

FIG. 8. Angle dependence of δf_{Ga}. The solid line is the fit using the Eq. (3). The inset shows the calculated angle dependence of the chemical shifts of the A and B molecules.

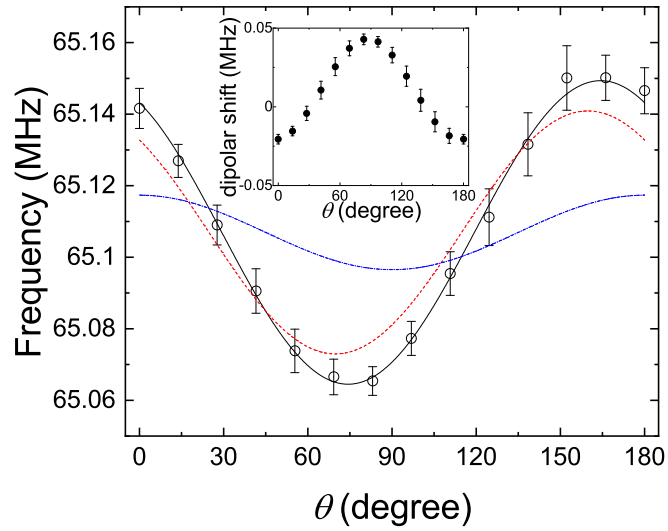

FIG. 9. Angle dependence of δf_{Fe}. The solid black line is the fit to the experimental data using the Eq. (6). The dashed red and blue lines represent the sine and cosine components of the fit, respectively. The inset shows the angular dependence of the dipolar shift.

Figure 7 shows the angle dependence of the NMR shift of λ-(BEDSe-TTF)$_2$GaCl$_4$ and λ-(BEDSe-TTF)$_2$FeCl$_4$ at 100 K. As the spectrum consists of four signals with slightly different hyperfine coupling constants, the error bar is not the standard deviation in the fitting parameter but is defined as one-fifth of the full width at half-maximum of the NMR spectrum.

The angular dependence of the resonance frequency of λ-(BEDSe-TTF)$_2$GaCl$_4$(f_{Ga}) is described as

$$f_{\mathrm{Ga}} = \gamma A_\pi(\theta)\chi_\pi H + \gamma[1+\sigma(\theta)]H, \tag{1}$$

where γ and χ_π are the gyromagnetic ratio and the magnetic susceptibility of the π spins, respectively; $A_\pi(\theta)$ is the hyperfine coupling constant of a π electron; and $\sigma(\theta)$ is the corresponding chemical shift. We can use λ-(BEDSe-TTF)$_2$GaCl$_4$ as a reference to evaluate the hyperfine coupling constant for the π spins ($A_\pi(\theta)$). As a chemical shift depends on the molecular structure and valence of a molecule, the chemical shift tensor of α-(BEDT-TTF)$_2$I$_3$ is used [29]. There are two crystallographically independent molecules in λ-type salts, but their chemical shifts are almost the same, as shown in the inset of Fig. 8. Hence, we used the mean value of the calculated chemical shifts for the two molecules. Subtracting the chemical shift from f_{Ga} yields δf_{Ga} as,

$$\delta f_{\mathrm{Ga}} = \gamma A_\pi(\theta)\chi_\pi H + \gamma H. \tag{2}$$

Here, γH is determined from the resonance frequency of tetramethylsilane (TMS). δf_{Ga} reaches a minimum at approximately 70°. Figure 1(b) shows that the 70° corresponds to the angle parallel to the molecular plane (perpendicular to the p_z orbital). As $A_\pi(\theta)$ consists of isotropic (A_π^{iso}) and anisotropic (A_π^{aniso}) terms, δf_{Ga} is described as follows:

$$\begin{aligned}\delta f_{\mathrm{Ga}} &= \gamma A_\pi^{\mathrm{iso}}\chi_\pi H + \gamma A_\pi^{\mathrm{aniso}}(\theta)\chi_\pi H + \gamma H \\ &= F_{\mathrm{Ga}}^{\mathrm{aniso}}\sin(2\theta - 2\alpha) + \mathrm{F}_{\mathrm{Ga}}^{\mathrm{iso}}.\end{aligned} \tag{3}$$

Using the equation presented above to fit the δf_{Ga} data yielded $F_{\mathrm{Ga}}^{\mathrm{aniso}} = 0.0268(8)$ MHz, $\alpha = 114.8(7)^\circ$, and $F_{\mathrm{Ga}}^{\mathrm{iso}} = 65.1200(6)$ MHz (Fig. 8).

The angular dependence of the NMR shift of λ-(BEDSe-TTF)$_2$FeCl$_4$ contains an additional 3d spin contribution, and the resonance frequency (f_{Fe}) can be described as

$$\begin{aligned}f_{\mathrm{Fe}} = {} & \gamma A_\pi(\theta)\chi_\pi(H + J_{\pi d,q=0}M_d) + \gamma[1+\sigma(\theta)]H \\ & + \gamma[H_{\mathrm{dip}}(\theta) + H_{\mathrm{demag}}(\theta)],\end{aligned} \tag{4}$$

where M_d, $H_{\mathrm{dip}}(\theta)$, and $H_{\mathrm{demag}}(\theta)$ are the magnetization of the 3d spins, dipolar fields from the surrounding 3d spins, and demagnetization contribution that depends on the crystal shape, respectively [25,26]. The magnetic moments of Fe ions, M_d, which are parallel to the external field, H, produce an exchange field on the π electrons through $J_{\pi d,q=0}$. The external field and exchange field polarize the π electrons corresponding to the first term in Eq. (4). In addition, the moments generate the dipolar field, H_{dip}, and the demagnetization field, H_{demag} corresponding to the third term in Eq. (4). The phase difference between the Ga and Fe salts originates from the third term.

The dipolar field generated by 3d spins can be calculated using the Lorentz method [25]. $H_{\mathrm{dip}}(\theta)$ was estimated by summing the dipole fields generated by the 3d spins in the Lorentz sphere with a radius of 30 Å. We found that $H_{\mathrm{dip}}(\theta)$ remains almost unchanged for Lorentz sphere radii above 30 Å and the four crystallographic independent sites have practically identical values of $H_{\mathrm{dip}}(\theta)$. Hence, we used the mean $H_{\mathrm{dip}}(\theta)$ over four sites as $H_{\mathrm{dip}}(\theta)$. We assumed M_d follows the Curie's law with $S = 5/2$ [20]. Using $M_d = 0.4761$ μ_{B} at 100 K, we calculated $H_{\mathrm{dip}}(\theta)$ with a standard deviation as the average of the dipole fields exerted on the four crystallographically nonequivalent ^{13}C sites shown in the inset of Fig. 9.

Our crystals were not perfect but mosaic. However, as the mosaic grain was considerably larger than 30 Å, we were

able to use $H_{\rm dip}(\theta)$. Subtracting the chemical shift and dipolar shifts from $F_{\rm Fe}$ yields the following equation:

$$\delta f_{\rm Fe} = \gamma A_\pi(\theta)\chi_\pi(H + J_{\pi d,q=0}M_d) + \gamma H_{\rm demag}(\theta) + \gamma H. \tag{5}$$

The first term is in phase with the Ga salt. $H_{\rm demag}(\theta)$ significantly affects the estimate of $J_{\pi d,q=0}$. Figure 2(b) shows that the rotation axis is the long axis of the thin rectangular crystal and $\theta = 0^\circ$ corresponds to the direction parallel to the crystal plane. As the demagnetization contribution depends on the crystal shape, the anisotropic part of $\gamma H_{\rm demag}(\theta)$ is in phase with $\cos 2\theta$.

As a result, we were able to fit $\delta f_{\rm Fe}$ using the following equation.

$$\delta f_{\rm Fe} = F_{\rm Fe}^{\rm aniso}\sin[2(\theta - 114.8)] + {\rm F}_{\rm demag}^{\rm aniso}\cos 2\theta + {\rm F}_{\rm Fe+demag}^{\rm iso}. \tag{6}$$

We obtained $F_{\rm Fe}^{\rm aniso} = 0.034(1)$ MHz, $F_{\rm demag}^{\rm aniso} = 0.010(1)$ MHz, and $F_{\rm Fe+demag}^{\rm iso} = 65.1069(5)$ MHz as the fitting parameters (Fig. 9).

Here, we examine the validity of our demagnetization parameters. In the previous studies, the demagnetization factor was not determined experimentally but roughly estimated as $H_{\rm demag}(\theta) = 4\pi M_z(1/3 - N_{a'}\cos^2\theta - N_{b^*}\sin^2\theta)$, where $N_{a'}$ and N_{b^*} are form factors, with $(N_{a'} + N_{b^*} \sim 1)$, by approximating the crystal outline as a rotating ellipsoid [25,26].

For λ-$(BETS)_2FeCl_4$, $N_{a'} = 0.2$ and $N_{b^*} = 0.8$ were used for a long thin rectangular crystal [25]. However, we estimated the factor by using the experimentally determined angle dependence of the shift of λ-$(BEDSe\text{-}TTF)_2FeCl_4$. The fitting parameter of $F_{\rm demag}^{\rm aniso} = 0.010(1)$ MHz corresponds to $N_{a'} = 0.35$ and $N_{b^*} = 0.65$, which are semiquantitatively consistent with the values for a long thin rectangular crystal.

Now, we investigate the difference in the coefficients of the first terms, $F_{\rm Fe}^{\rm aniso}$ and $F_{\rm Ga}^{\rm aniso}$. The ratio of the coefficients of the first terms is expressed below.

$$\frac{F_{\rm Fe}^{\rm aniso}}{F_{\rm Ga}^{\rm aniso}} = \frac{H + J_{\pi d,q=0}M_d}{H}. \tag{7}$$

We used the ratio to determine the exchange magnetic field $J_{\pi d,q=0}M_d$ as 1.6(4) T at 100 K and $J_{\pi d,q=0}$ in λ-$(BEDSe\text{-}TTF)_2FeCl_4$ as 3.4(7) T/μ_B . The absolute value of |3.4(7)| T/μ_B is smaller than that of λ-$(BETS)_2FeCl_4$, (|−6.6| T/μ_B), which is consistent with the prediction in our previous study.

C. Path of the π-d interaction

Figure 10(a) is a schematic of $J_{\pi\pi}$, $J_{\pi d}$, and J_{dd} in π-d systems. Here, $J < 0$ corresponds to an AF interaction and $J > 0$ corresponds to a ferromagnetic interaction. A π-d system generally consists of two spin systems interacting with $J_{\pi d}$, an $S = 1/2$ system interacting with $J_{\pi\pi}$, and an $S = 5/2$ system interacting with J_{dd}. The AF transition in λ-$(BEDSe\text{-}TTF)_2FeCl_4$ is confirmed to occur in the donor layers, as in λ-$(BEDSe\text{-}TTF)_2GaCl_4$, and J_{dd} is expected to be smaller than $J_{\pi\pi}$ [28].

Figure 1(a) shows that the inner and outer chalcogen atoms in BEDSe-TTF molecules are S and Se atoms, respectively.

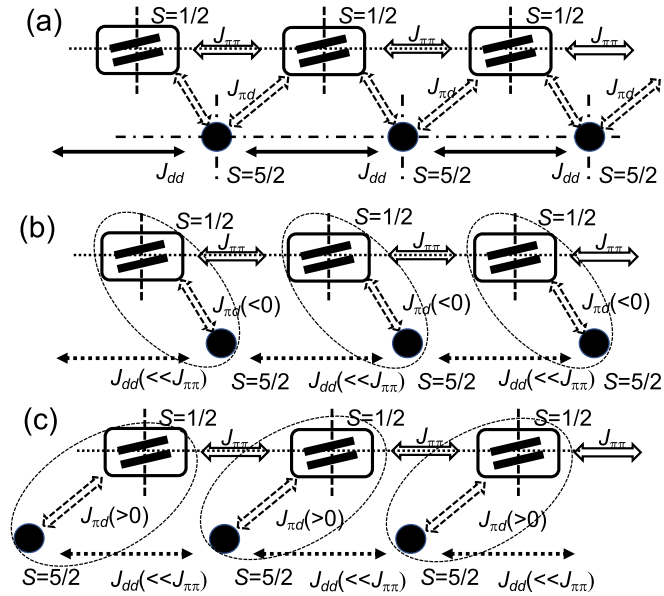

FIG. 10. Schematic of $J_{\pi\pi}$, $J_{\pi d}$, and J_{dd} in (a) π-d systems, (b) λ-$(BETS)_2FeCl_4$, and (c) λ-$(BEDSe\text{-}TTF)_2FeCl_4$. Molecules and anions are represented by thick lines and circles, respectively.

This placement of chalcogen atoms is reversed from that in the BETS molecules. There are two π-d interaction paths: through the inner chalcogen atoms and through the outer chalcogen atoms. The shortest S-Cl contact is usually shorter than the shortest Se-Cl contact because the ionic radius of S is smaller than that of Se. However, as for the path of the π-d interaction shown in Fig. 11, the Se-Cl contact in λ-$(BETS)_2FeCl_4$ of 3.4691(10) Å is shorter than the S-Cl contact in λ-$(BEDSe\text{-}TTF)_2FeCl_4$ of 3.5678(13) Å [20,30]. By contrast, the distance between the outer chalcogen (Se) and Cl in λ-$(BEDSe\text{-}TTF)_2FeCl_4$ is 3.2421(8) Å and smaller than the corresponding distance of S-Cl in λ-$(BETS)_2FeCl_4$ of 3.3855(10) Å. These results suggest that the Se-Cl contacts are the main contribution to the π-d interaction. Hence, the dominant interaction path is through the inner chalcogen atom

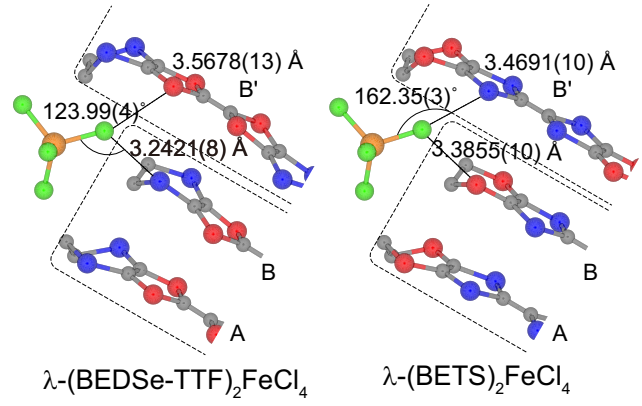

FIG. 11. Short contact between Cl and the chalcogen and the angle formed by Fe···Cl···chalcogen atom in λ-$(BEDSe\text{-}TTF)_2FeCl_4$ and λ-$(BETS)_2FeCl_4$. A, B, and B′ molecules are defined in Fig. 1(b).

in λ-$(BETS)_2FeCl_4$ and through the outer chalcogen atom in λ-$(BEDSe\text{-}TTF)_2FeCl_4$ because the 3*d* spins of Fe are expected to interact with molecular dimers through Fe-Cl-Se contacts.

We discuss the relationship between $J_{\pi d,q=0}$ and $J_{\pi d,q=Q}$ in λ-$FeCl_4$ salts. Based on the discussion in Sec. III B, we should use the $J_{\pi d,q=Q}$ and not $J_{\pi d,q=0}$ for the AF state under the low fields. However, in λ-$FeCl_4$ salts, the paramagnetic 3*d* spins are not attached to the $S = 1/2$ system via the multipass $J_{\pi d}$ interaction, but to the nearest dimer via the single-pass $J_{\pi d}$ through the short Se-Cl contact, as shown in Figs. 10(b) and 10(c), because the Fe-Cl-Se contacts dominate the interaction path. Hence, $J_{\pi d,q=0}$ can be approximated as $J_{\pi d,q=0} \sim J_{\pi d}^{\text{Se-Cl}}$ and $|J_{\pi d,q=Q}|$ is almost equal to $|J_{\pi d}^{\text{Se-Cl}}|$. Here, $J_{\pi d}^{\text{Se-Cl}}$ is the exchange interaction between $FeCl_4^-$ and the connected dimer with a short Se-Cl contact. Namely, the units in which the π spin on a dimer are connected to the 3*d* spin via $J_{\pi d}$ interact with each other via $J_{\pi\pi}$ modeled in the π ordering scenario. The difference between λ-$(BETS)_2FeCl_4$ and λ-$(BEDSe\text{-}TTF)_2FeCl_4$ is that $FeCl_4^-$ ions interact with different dimers.

We previously reported that the π-*d* interaction of λ-$(BEDSe\text{-}TTF)_2FeCl_4$ is weaker than that of λ-$(BETS)_2FeCl_4$ [20]. As the 3*d* spins are paramagnetic, the absolute value of $J_{\pi d}$ results in an internal field being exerted on $FeCl_4^-$ and affects the magnetism under low fields. Indeed, λ-$(BEDSe\text{-}TTF)_2FeCl_4$ exhibits the same magnetization behavior as λ-$(BETS)_2FeBr_xCl_{4-x}$ with a weakened $J_{\pi d}$. The result of $|J_{\pi d,q=0}|_{\text{BETS}} > |J_{\pi d,q=0}|_{\text{BEDSe-TTF}}$ is consistent with previous speculation.

There is an extremely short distance between Se (the outer chalcogen atom) and Cl in λ-$(BEDSe\text{-}TTF)_2FeCl_4$, whereas there is a short distance between Se (the inner chalcogen atom) and Cl in λ-$(BETS)_2FeCl_4$. Considering with $|J_{\pi d,q=0}|_{\text{BETS}} > |J_{\pi d,q=0}|_{\text{BEDSe-TTF}}$, the interaction path through the inner chalcogen is essential for the π-*d* interaction. Theoretical calculations also suggest that the contact between the inner chalcogen atoms and Cl is important for the π-*d* interaction [28].

Next, we discuss the difference in the signs of $J_{\pi d}$. The $FeCl_4^-$ anion mainly interacts with different dimers in λ-$(BETS)_2FeCl_4$ and λ-$(BEDSe\text{-}TTF)_2FeCl_4$. As shown in Fig. 11, the angle of $Fe\cdots Cl\cdots$ (the inner chalcogen atom) in λ-$(BETS)_2FeCl_4$ is 162.35(3)° [30]. By comparison, the angle of $Fe\cdots Cl\cdots$ (the outer chalcogen atom) in λ-$(BEDSe\text{-}TTF)_2FeCl_4$ is 123.99(4)° [20]. As the sign of the exchange interaction depends on the angle of the interaction path, the difference in the angles could explain the difference in the signs of $J_{\pi d}$ [31].

Numerous salts containing S-based donors and magnetic ions have been synthesized, but no distinct π-*d* interactions have been reported. This result suggests that the introduction of Se increases both the dimensionality of the conducting layer and the strength of the interaction between donor molecules and counteranions as evidenced by the extremely short Se-Cl contact compared to S-Cl contact. TMTSF and BEDSe-TTF salts containing Se, as well as BETS salts, are potential candidates for investigating π-*d* systems. Our quantitative $J_{\pi d}$ evaluation, including the demagnetization contribution, could be applied to various π-*d* systems. The Bechgaard salts have a rich phase diagram including spin density wave (SDW) and SC, with PF_6^- and ClO_4^- as anions [32]. Our results suggest the possibility of extending the π-*d* interaction to the well-studied Bechgaard salts, and the interactions of the *d*-electron with the SDW and SC will be of interest.

IV. SUMMARY

We performed ^{13}C NMR measurements on λ-$(BEDSe\text{-}TTF)_2FeCl_4$. Spectral splitting and the divergence of $1/T_1$ toward 25 K suggest that the AF transition in donor layers occurs at 25 K. The magnetic structure in the AF phase resembles that of λ-$(BEDSe\text{-}TTF)_2GaCl_4$. We experimentally determined $J_{\pi d}$ for λ-$(BEDSe\text{-}TTF)_2FeCl_4$ as 3.4(7) T/μ_B from the angle dependence of the NMR shift of the paramagnetic phase. The absolute value of $J_{\pi d}$ is smaller than that of λ-$(BETS)_2FeCl_4$, which is consistent with our previous conclusion based on the anisotropic magnetization at low fields. The sign of $J_{\pi d}$ in λ-$(BEDSe\text{-}TTF)_2FeCl_4$ is opposite to that of λ-$(BETS)_2FeCl_4$. The differences in the absolute value and sign of $J_{\pi d}$ may originate from the difference in Fe-Cl-Se contacts between λ-$(BEDSe\text{-}TTF)_2FeCl_4$ and λ-$(BETS)_2FeCl_4$.

ACKNOWLEDGMENTS

We thank A. Ito for the sample preparation of λ-$(BEDSe\text{-}TTF)_2GaCl_4$. This work was supported by JST SPRING, Grant No. JPMJSP2119 and Japan Society for the Promotion of Science KAKENHI Grants No. 20K14401 and No. 23K04685.

[1] R. H. McKenzie, Similarities between organic and cuprate superconductors, Science **278**, 820 (1997).

[2] A. Kobayashi, T. Udagawa, H. Tomita, T. Naito, and H. Kobayashi, New organic metals based on bets compounds with MX_4^- anions (BETS = bis (ethylenedithio)tetraselenafulvalene; M = Ga, Fe, In; X = Cl, Br), Chem. Lett. **22**, 2179 (1993).

[3] M. Tokumoto, T. Naito, H. Kobayashi, A. Kobayashi, V. N. Laukhin, L. Brossard, and P. Cassoux, Magnetic anisotropy of organic conductor λ-$(BETS)_2FeCl_4$, Synth. Met. **86**, 2161 (1997).

[4] L. Brossard, R. Clerac, C. Coulon, M. Tokumoto, T. Ziman, D. K. Petrov, V. N. Laukhin, M. J. Naughton, A. Audouard, F. Goze, A. Kobayashi, H. Kobayashi, and P. Cassoux, Interplay between chains of S = 5/2 localised spins and two-dimensional sheets of organic donors in the synthetically built magnetic multilayer λ-$(BETS)_2FeCl_4$, Eur. Phys. J. B **1**, 439 (1998).

[5] H. Akiba, S. Nakano, Y. Kajita, B. Zhou, A. Kobayashi, and H. Kobayashi, Mysterious paramagnetic states of fe 3d spin in antiferromagnetic insulator of λ-$BETS_2FeCl_4$ system, J. Phys. Soc. Jpn. **78**, 033601 (2009).

[6] H. Akiba, K. Nobori, K. Shimada, Y. Nishio, K. Kajita, B. Zhou, A. Kobayashi, and H. Kobayashi, Magnetic and thermal properties of λ-$(BETS)_2FeCl_4$ system -Fe 3*d* spin in antiferromagnetic insulating phase-, J. Phys. Soc. Jpn. **80**, 063601 (2011).

[7] M. A. Tanatar, T. Ishiguro, H. Tanaka, and H. Kobayashi, Magnetic field-temperature phase diagram of the quasi-two-dimensional organic superconductor λ-$(BETS)_2GaCl_4$ studied via thermal conductivity, Phys. Rev. B **66**, 134503 (2002).

[8] S. Uji, K. Kodama, K. Sugii, T. Terashima, T. Yamaguchi, N. Kurita, S. Tsuchiya, T. Konoike, M. Kimata, A. Kobayashi, B. Zhou, and H. Kobayashi, Vortex dynamics and diamagnetic torque signals in two dimensional organic superconductor λ-$(BETS)_2GaCl_4$, J. Phys. Soc. Jpn. **84**, 104709 (2015).

[9] H. Mori, T. Okano, M. Kamiya, M. Haemori, H. Suzuki, S. Tanaka, Y. Nishio, K. Kajita, and H. Moriyama, Bandwidth and band filling control in organic conductors, Physica C: Superconductivity **357–360**, 103 (2001).

[10] H. Mori, H. Suzuki, T. Okano, H. Moriyama, Y. Nishio, K. Kajita, M. Kodani, K. Takimiya, and T. Otsubo, Positional order and disorder of symmetric and unsymmetric BEDT-STF salts, J. Solid State Chem. **168**, 626 (2002).

[11] T. Minamidate, H. Shindo, Y. Ihara, A. Kawamoto, N. Matsunaga, and K. Nomura, Role of the *d*-*d* interaction in the antiferromagnetic phase of λ-$(BEDT\text{-}STF)_2FeCl_4$, Phys. Rev. B **97**, 104404 (2018).

[12] S. Fukuoka, T. Minamidate, Y. Ihara, and A. Kawamoto, Selective observation of sublattice magnetization in the molecular π-*d* system λ-$(BEDT\text{-}STF)_2FeCl_4$ studied by ^{13}C NMR, Phys. Rev. B **101**, 184402 (2020).

[13] S. Fukuoka, M. Sawada, T. Minamidate, N. Matsunaga, K. Nomura, Y. Ihara, A. Kawamoto, Y. Doi, M. Wakeshima, and Y. Hinatsu, Multistep development of the hyperfine fields in λ-$(BEDT\text{-}STF)_2FeCl_4$ studied by Mössbauer spectroscopy, J. Phys. Soc. Jpn. **87**, 093705 (2018).

[14] S. Fukuoka, T. Minamidate, N. Matsunaga, Y. Ihara, and A. Kawamoto, Thermodynamic investigation on antiferromagnetic ordered state of the molecular π-*d* system λ-$(BEDT\text{-}STF)_2FeCl_4$, J. Phys. Soc. Jpn. **89**, 073704 (2020).

[15] Y. Saito, H. Nakamura, M. Sawada, T. Yamazaki, S. Fukuoka, N. Matsunaga, K. Nomura, M. Dressel, and A. Kawamoto, Disordered quantum spin state in the stripe lattice system consisting of triangular and square tilings, arXiv:1910.09963v2.

[16] T. Minamidate, Y. Oka, H. Shindo, T. Yamazaki, N. Matsunaga, K. Nomura, and A. Kawamoto, Superconducting phase in λ-$(BEDT\text{-}STF)_2GaCl_4$ at high pressures, J. Phys. Soc. Jpn. **84**, 063704 (2015).

[17] T. Minamidate, D. P. Sari, N. Matsunaga, and I. Watanabe, Muon spin relaxation study on the new organic spin liquid material λ-$(STF)_2GaCl_4$, RIKEN Accel. Prog. Rep. **51**, 205 (2018).

[18] Y. Saito, S. Fukuoka, T. Kobayashi, A. Kawamoto, and H. Mori, Antiferromagnetic ordering in organic conductor λ-$(BEDT\text{-}TTF)_2GaCl_4$ probed by ^{13}C NMR, J. Phys. Soc. Jpn. **87**, 013707 (2018).

[19] A. Ito, T. Kobayashi, D. P. Sari, I. Watanabe, Y. Saito, A. Kawamoto, H. Tsunakawa, K. Satoh, and H. Taniguchi, Antiferromagnetic ordering of organic Mott insulator λ-$(BEDSe\text{-}TTF)_2GaCl_4$, Phys. Rev. B **106**, 045114 (2022).

[20] R. Saito, Y. Iida, T. Kobayashi, H. Taniguchi, N. Matsunaga, S. Fukuoka, and A. Kawamoto, Magnetic state in the quasi-two-dimensional organic conductor λ-$(BEST)_2FeCl_4$ and the path of π-*d* interaction, Phys. Rev. B **105**, 165115 (2022).

[21] H. Akutsu, K. Kato, E. Ojima, H. Kobayashi, H. Tanaka, A. Kobayashi, and P. Cassoux, Coupling of metal-insulator and antiferromagnetic transitions in the highly correlated organic conductor incorporating magnetic anions, λ-$BETS_2FeBr_xCl_{4-x}$ [BETS = Bis(ethylenedithio)tetraselenafulvalene], Phys. Rev. B **58**, 9294 (1998).

[22] V. Jaccarino and M. Peter, Ultra-High-Field Superconductivity, Phys. Rev. Lett. **9**, 290 (1962).

[23] S. Uji, H. Shinagawa, T. Terashima, T. Yakabe, Y. Terai, M. Tokumoto, A. Kobayashi, H. Tanaka, and H. Kobayashi, Magnetic-field-induced superconductivity in a two-dimensional organic conductor, Nature (London) **410**, 908 (2001).

[24] L. Balicas, J. S. Brooks, K. Storr, S. Uji, M. Tokumoto, H. Tanaka, H. Kobayashi, A. Kobayashi, V. Barzykin, and L. P. Gor'kov, Superconductivity in an Organic Insulator at Very High Magnetic Fields, Phys. Rev. Lett. **87**, 067002 (2001).

[25] K. Hiraki, H. Mayaffre, M. Horvatić, C. Berthier, S. Uji, T. Yamaguchi, H. Tanaka, A. Kobayashi, H. Kobayashi, and T. Takahashi, ^{77}Se NMR evidence for the jaccarino-peter mechanism in the field induced superconductor, λ-$(BETS)_2FeCl_4$, J. Phys. Soc. Jpn. **76**, 124708 (2007).

[26] S. Fukuoka, Y. Ito, Y. Ihara, and A. Kawamoto, ^{13}C NMRstudy of the stabilization of the antiferromagnetic ground state and the emergence of unconventional magnetic state in a molecular π-*d* system, Phys. Rev. B **105**, 134427 (2022).

[27] S. Fujiyama, M. Takigawa, J. Kikuchi, H. B. Cui, H. Fujiwara, and H. Kobayashi, Compensation of Effective Field in the Field-Induced Superconductor κ-$(BETS)_2FeBr_4$ Observed by ^{77}Se NMR, Phys. Rev. Lett. **96**, 217001 (2006).

[28] T. Mori and M. Katsuhara, Estimation of πd-interactions in organic conductors including magnetic anions, J. Phys. Soc. Jpn. **71**, 826 (2002).

[29] T. Kawai and A. Kawamoto, ^{13}C-NMR study of charge ordering state in the organic conductor, α-$(BEDT\text{-}TTF)_2I_3$, J. Phys. Soc. Jpn. **78**, 074711 (2009).

[30] T. Lee, Y. Oshima, H. Cui, and R. Kato, Detailed x-band studies of the π-*d* molecular conductor λ-$(BETS)_2FeCl_4$: Observation of anomalous angular dependence of the g-value, J. Phys. Soc. Jpn. **87**, 114702 (2018).

[31] J. Kanamori, Superexchange interaction and symmetry properties of electron orbitals, J. Phys. Chem. Solids **10**, 87 (1959).

[32] D. Jérome, The physics of organic superconductors, Science **252**, 1509 (1991).